

# Mechanical-Based Design for Airfoil Structural Morphing

Mattia Butera\*, Amanda Butler\*, Amiri Hayes\*, Evan Schaffer\*, Niti Sinha\*  
Jay Kapasiawala<sup>†</sup> and Dr. Prosenjit Bagchi<sup>†</sup>

\*The New Jersey Governor's School of Engineering and Technology, Rutgers University–New Brunswick, NJ, USA

<sup>†</sup>Corresponding Author

Emails: {mattia.t.butera, fofochiab, amirihayes1, evanschaffer, nitisinha0829}@gmail.com  
{jk1695@rutgers.edu, pbagchi@soe.rutgers.edu}

**Abstract**—Conventionally, airfoils are designed to work optimally in specific regimes of flight. However, using one fixed wing across different regimes of speed such as those above the speed of sound (supersonic) and those below (subsonic), causes inefficient flight. Supersonic airfoils do not generate enough lift to be used effectively at subsonic speeds and subsonic airfoils generate more drag than lift at supersonic speeds. The ideal airfoil maximizes lift while minimizing drag; thus, a morphing airfoil was designed to enable a more efficient transition from subsonic to supersonic flight. A prototype was constructed to demonstrate a possible mechanism which changes airfoil geometry mid-flight. The design was tested using computer software, Ansys and COMSOL, in addition to calculations of aerodynamic equations, which ultimately revealed the effectiveness of the morphing airfoil in multiple flight regimes.

## I. INTRODUCTION

### A. Overview

The rapid modernization of the aviation industry has incited widespread interest in aircraft with the ability to achieve supersonic speeds. The notion of improved performance and sustainability has incentivized manufacturers to design aircraft which can fly at supersonic speeds without deleterious effects on fuel efficiency, noise pollution, or smog. While subsonic speeds are considerably easier to design around, the aircraft industry intends to progress towards a future with reduced flight time and emissions. An airfoil is a two-dimensional representation of the cross-sectional area of an aircraft wing; different airfoil geometries have a profound impact on the efficiency of the aircraft.

### B. Motivation

If the wing geometry is inappropriate for the flight regime, as the aircraft approaches supersonic speeds, drag divergence—where the force that prevents flight (drag) increases rapidly—occurs. Contrary to supersonic airfoils, airfoils designed to maximize lift in subsonic flight are generally thicker and rounder, which forms an intense shockwave at supersonic speeds and an increased amount of flow separation, increasing drag and decreasing efficiency [1]. Hence, subsonic and supersonic aircraft are two separate categories and require distinct airfoil geometries. For aircraft to traverse these flight regimes efficiently, a mid-flight modification of the airfoil is required. Computer simulations, principal aerodynamics calculations, and construction of an airfoil prototype with

dynamic geometry were effectively implemented in this design for an amorphous airfoil.

## II. BACKGROUND

### A. Aerodynamic Efficiency

Lift and drag are the two prime forces influencing flight; lift enables flight while drag resists it. The coefficients of lift and drag are non-dimensionalized values derived from lift and drag.

Lift, the upward force exerted on the wing, opposes the downward gravitational force and allows for flight. For airfoils, the lift force  $L$  is equal to the product of the air density  $\rho$ , freestream velocity  $V_\infty$ , and the air circulation  $\Gamma$ .

$$L = \rho V_\infty \Gamma \quad (1)$$

How much lift an airplane can generate depends on the wing geometry, consisting of chord length, angle of attack (AOA), camber, shape of the wing, and the ratio of wing span to wing area.

Drag is a force exerted horizontally towards the rear of the airfoil, opposing forward motion. Induced drag, caused by downwash (the downward diversion of the incoming airstream caused by an aircraft wing), is the most fundamental type of drag to consider in aerodynamics at both subsonic and supersonic speeds [1]. At supersonic speeds, the friction due to air viscosity (a fluid's resistance to flow) increases, causing wave drag. Flow separation causes a section of recirculating air with low velocity above the wing. As a result of Bernoulli's principle, increased pressure above the wing is created, resulting in wave drag.

$$D_i = L \sin \alpha_i \quad (2)$$

Equation (2) describes induced drag force ( $D_i$ ) as a function of lift force  $L$  and the angle of attack  $\alpha$ . Using these values of lift and drag, coefficients of lift and drag were then calculated.

$$c_L = \frac{L}{\frac{1}{2} \rho V_\infty l} \quad (3)$$

$$c_D = \frac{D}{\frac{1}{2} \rho V_\infty l} \quad (4)$$

Lift and drag are correlated; as lift increases, drag increases. When the speed of an airplane is slower than the speed of

sound (343 m/s), it is optimal for the shape of the airfoil to resemble an asymmetric, horizontal teardrop (see Figure 1). At supersonic speeds, the shape of the airfoil must be thinner, which sacrifices lift, but decreases a significant amount of drag [1].

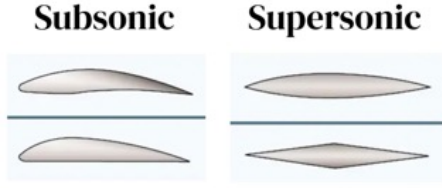


Fig. 1. Subsonic Airfoil Geometry Versus Supersonic Airfoil Geometry [2]

Another essential factor to consider is the angle of attack. Increasing the AOA generally increases lift as well as induced drag. This trend only continues until 15-20 degrees, at which point lift is lost because airflow across the upper side of the airfoil becomes detached in an event identified as stall. It is essential to obtain a proper AOA which maximizes lift without causing stall [3]. Simulations for this paper were conducted at a 10-degree AOA.

### B. Quantifying Lift and Drag

A static airfoil optimized for subsonic flight is not fit for supersonic flight and vice versa [4]. In order to calculate values of lift and drag to confirm this, simulations in COMSOL and Ansys were used. An airfoil that can morph efficiently would get thinner as speed increases and take advantage of increasing values of lift from thinner airfoils in the supersonic regime.

### C. Existing Research

Currently, the majority of aircraft are designed to perform most efficiently within a specific environment. Designing a mechanism in which the airfoil shape could morph would overcome these issues to develop a more versatile aircraft. Existing solutions that have been developed include the use of shape memory alloys (SMAs) and machinery which twists, bends, or rotates the wing. SMAs are metals or alloys purposefully deformed and can return to their initial state when heated [5]. The other type of morphing proposed is machinery inside the wing, which often employ motor-based systems. Both of these solutions have been implemented only in prototypes.

## III. PROCEDURE

### A. A Mechanical Approach

To allow for a more efficient flight, a morphing airfoil with changing geometry was constructed. A design with a cam system driven by a NEMA-17 stepper motor was selected; a cam converts rotational motion, in this case from the stepper motor, into linear motion. The flexible material for the airfoil selected was fiberglass combined with epoxy so that the rotation of the cam would allow the geometry of the airfoil to change.

### B. COMSOL, Ansys, and MATLAB

The two pieces of software used to create computer simulations for airfoils were COMSOL Multiphysics and Ansys. They are ideal platforms that use computational fluid dynamics to model airfoils; they return values such as lift force ( $L$ ) and drag force ( $D$ ), and are capable of generating pressure and velocity graphs. These values were also calculated individually using MATLAB to introduce another layer of accuracy.

1) *COMSOL*: COMSOL software was implemented to simulate subsonic flight. The extended set of points that makes up the airfoil point-curve was found online at Airfoil Tools and imported as an interpolation curve using a table. *Laminar Flow simulation* was selected to input the necessary parameters and aerodynamic equations into the software. Parameters for pressure, velocity, temperature, and AOA were specified, and simulation was generated. Further, tables were generated by specifying quantities (such as lift force) to calculate. It is important to note that subsonic speed simulations were created in COMSOL due to the software being more effective for this flight regime than Ansys [1].

2) *Ansys*: Supersonic flight was simulated in CFD software, Ansys. A .STEP file of the desired airfoil geometry was imported into the geometry of an Ansys Fluid Flow (fluent) file. After the geometry was edited and a mesh was created, a viscous model was created in a density based simulation. The environmental conditions were set, and after initializing the simulations, calculations were stated to generate specified quantities (such as lift and drag forces), along with a pressure contour graph.

3) *MATLAB*: After simulating the airfoils, MATLAB was used to calculate the coefficients of lift and drag. Aerodynamic equations were employed which declared lift as a function using the following equations:

$$c_L = 2\pi(1 + \frac{4}{3\sqrt{3}})(\frac{t}{l})\alpha \quad (5)$$

$$c_{Di} = \frac{L\alpha}{\frac{1}{2}\rho v^2 l} \quad (6)$$

$$c_{Df} = \frac{D_f}{\frac{1}{2}\rho v^2 l} \quad (7)$$

where  $\alpha$  is AOA in radians,  $t$  is the max thickness of the airfoil in meters,  $l$  is the chord length in meters,  $v$  is free stream velocity in meters per second,  $\rho$  is air density in grams per cubic meter,  $D$  is drag in Newtons, and  $L$  is lift in Newtons. The values for  $L$  and  $D$  are derived from Equations (1) and (2). The coefficients of lift and drag were calculated using MATLAB, graphed, and compared with the simulated values at multiple angles of attack to corroborate information about the efficiency of the airfoil.

In addition, fuel efficiency for considered airfoils was calculated to confirm that the amorphous design was more sustainable than non-morphing airfoils. Calculating the fuel efficiency ensures that the weight of the aircraft as a whole—including the motor, cam, and other components—still demands less fuel

than current alternatives. Fuel efficiency was calculated using the following kinematic equations:

$$D = \frac{c_D \rho v^2 A_1}{2} \quad (8)$$

$$L = \frac{c_L \rho v^2 A_2}{2} \quad (9)$$

where  $v$  is the velocity of the aircraft,  $A_1$  is the cross sectional area of the airfoil, and  $A_2$  is the planform area of the wing. It is important to note that lift and drag in Equations (8) and (9) are for the entire aircraft rather than solely the airfoil. The aircraft's lift, drag, thrust, and weight at supersonic and subsonic speeds were then used in kinematic equations to determine the number of gallons consumed per mile.

### C. Final Airfoil Model

The airfoil of the subsonic P-51 Mustang, the BL17.5, was chosen because of its lesser thickness (16.5%), relative to other subsonic airfoils. Similarly, the airfoil of the supersonic F-16 Fighting Falcon, the NACA 64-206, was chosen due to its similar dimensions to the subsonic airfoil [6-7]. The airfoils were proportioned to one another according to their perimeters. The final model preserved the same surface area but changed thickness, camber, and chord length.

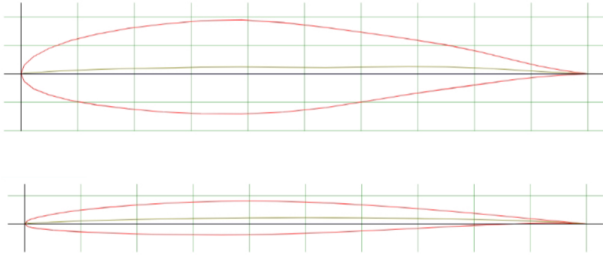


Fig. 2. (top) BL17.5 subsonic and (bottom) NACA 64-206 supersonic airfoils [8-9]

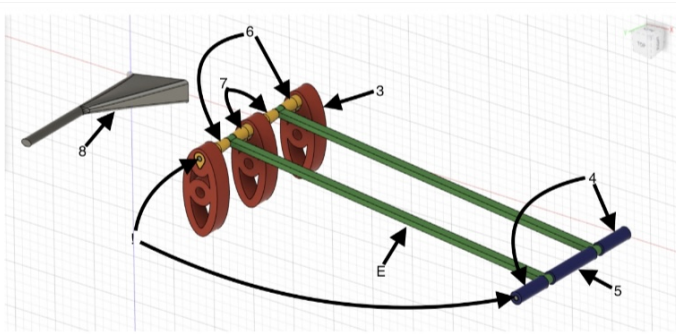


Fig. 3. Fusion 360 Cam System

The prototype was constructed by employing 3D printing and laser cutting, and built with materials such as fiberglass and epoxy. Despite an airfoil being a two-dimensional

representation of an airplane wing, the physical prototype contained necessary internal structure to provide depth to create a wing (see figure 3). The width of the elliptical cam would correspond to the supersonic airfoil thickness, and the height to the subsonic airfoil thickness (see figure 2). To provide structure to the trailing edge, a connecting rod was anchored at a point on the cam; as the airfoil thickened, the chord length of the airfoil diminished.

TABLE I  
AIRFOIL DIMENSIONS

| Aircraft                   | BL17.5  | NACA 64-206 |
|----------------------------|---------|-------------|
| Chord length [m]           | 0.35    | 0.335164    |
| Max thickness [% of chord] | 16.5    | 6           |
| M.T. location [% of chord] | 38.9    | 40          |
| Max thickness[m]           | 0.05775 | 0.020109    |
| M.T. location [m]          | 0.13615 | 0.134065    |
| Max camber [% of chord]    | 1.3     | 1.1         |
| M.C. location [% of chord] | 68.3    | 50          |
| Max camber [m]             | 0.00455 | 0.003687    |
| M.C. location [m]          | 0.23905 | 0.167582    |

## IV. RESULTS

### A. Physical Airfoil Performance

The final physical airfoil prototype was composed of the cam mechanism (Fig. 3), the fiberglass-epoxy airfoil, and an acrylic, laser-cut baseboard to house the stepper motor. The stepper motor successfully rotated the cam 90 degrees counterclockwise from the vertical (subsonic) position to the horizontal (supersonic) position. The fiberglass-epoxy combination flexed with the movement of the cam. Meanwhile, the cam mechanism changed the chord length, thickness, and camber of the airfoil, demonstrating the viability of an amorphous airfoil.

### B. Simulation Proof

COMSOL and Ansys simulations each used typical flight environments. Atmospheric pressure was standardized across experiments at a constant 54000 Pa, and atmospheric temperature was standardized at a constant 242K, or -31.15 degrees Celsius. These parameters model ideal passenger flight conditions [10]. Subsonic simulations were tested at 100 m/s, well within the subsonic range and well below the transonic flow region, which begins at Mach 0.8 (274.4 m/s). Similarly, supersonic simulations were tested at Mach 3.5 (1200.5 m/s), well above the supersonic and transonic flow cutoff, which ends at about Mach 1.2 (411.6 m/s). The AOA was also standardized at ten degrees, though data was collected at zero degrees as well. The simulations proved that a subsonic airfoil (the BL17.5) is able to generate more lift in a subsonic environment than a supersonic airfoil (the NACA 64-206), and a supersonic airfoil generates less drag in a supersonic environment than a subsonic airfoil.

1) *BL17.5 Simulations:* Figure 4 demonstrates the BL17.5 at subsonic speed with a 10 degree AOA. When tested in COMSOL at 100 m/s, the BL17.5 airfoil generated 1147.46% greater lift force than the generated drag force of 208.54 N (see Table 2). Airstream velocity at the upper leading edge was much greater than below the airfoil, generating lift.

TABLE II  
BL17.5 VALUES FROM SIMULATION AND CALCULATION

| BL17.5              | AOA | 100[m/s] | Mach 0.6 |
|---------------------|-----|----------|----------|
| chord length [m]    |     | 1.0      | 1.0      |
| lift force [N]      | 0   | -529.46  | -2251    |
|                     | 10  | 2348.40  | 10001    |
| drag force [N]      | 0   | 287.06   | 1215.1   |
|                     | 10  | 695.61   | 2943.20  |
| Coefficient of Lift | 0   | -0.09    | -0.06    |
|                     | 10  | 0.38     | 0.26     |
| Coefficient of Drag | 0   | 0.05     | 0.03     |
|                     | 10  | 0.11     | 0.08     |

The BL17.5 airfoil would be ineffective at supersonic speeds because it would generate a high amount of wave drag. The thickness of the BL17.5 is too great for supersonic speeds; the most optimal airfoil found was the NACA 64-206 [11].

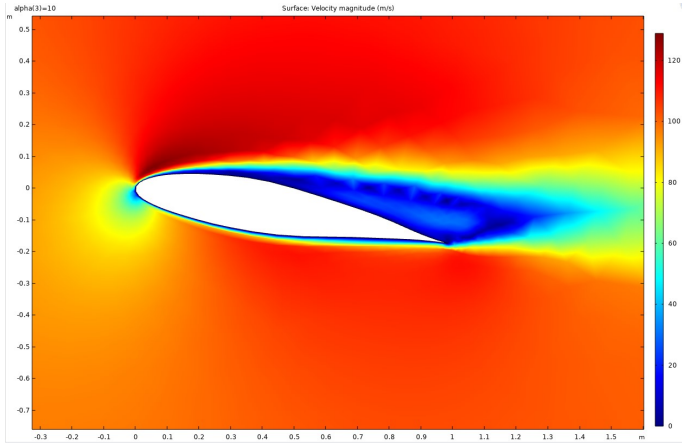


Fig. 4. BL17.5 with 10 degree AOA at 100m/s (from COMSOL)

2) *NACA 64-206 Simulations:* When tested in Ansys at Mach 3.5 (see figure 5), the NACA 64-206 airfoil generated 368.6% greater lift force than the generated drag force of 637928.3 N (see Table 3). The highest pressure is visible below the airfoil, while the lowest is visible above the airfoil; this generates lift. The triangular contour displays the existence of a shockwave, which is inevitable at supersonic speeds. When tested in COMSOL at 100 m/s (see figure 6), the NACA 64-206 generated a significantly smaller force of lift (3693.8 N), compared to the corresponding supersonic lift force (2351798 N) (see Table 3). Drag force of the NACA 64-206 followed a similar pattern. The NACA 64-206 was most effective at supersonic speeds.

### C. MATLAB

The coefficients of lift and drag were simultaneously calculated in MATLAB with aerodynamics equations (5), (6), and

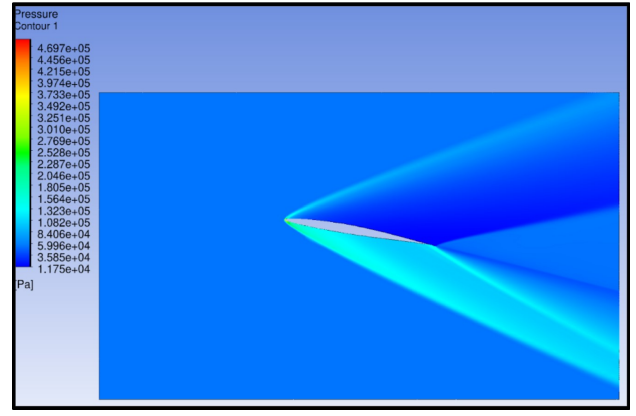


Fig. 5. NACA 64-206 at Mach 3.5 with 10 degree AOA

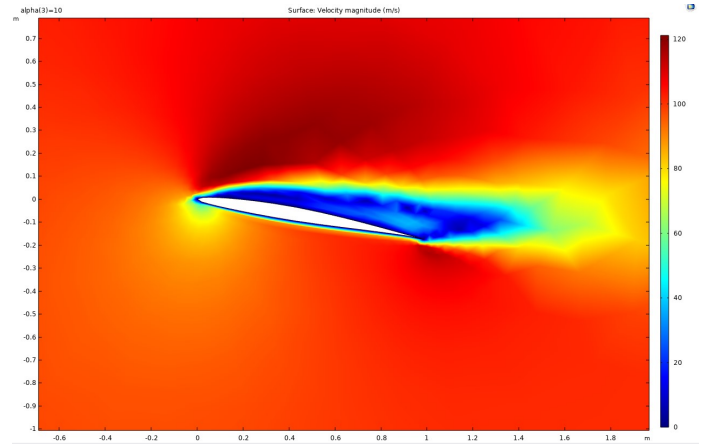


Fig. 6. NACA 64-206 at 100[m/s] with 10 degree AOA

(7). Programs were created to graph simulations and obtain experimental values for coefficient of lift and coefficient of friction against simulation obtained values [12]. Theoretical values were generally higher than experimental values, which means values derived using aerodynamic equations were more likely to overestimate values of lift and drag associated with airfoil geometries. Even so, the data still clearly showed that higher values for lift and lower values for drag were achieved with the two airfoils used in the morphing design.

Additionally, the fuel consumption graphs showed that the BL17.5 and NACA 64-206 airfoils used less fuel when the wing changed from one to the other. Data were collected about the aircraft the morphing wing would be attached to and used to approximate the fuel efficiency [12]. Then, the morphing aircraft was compared to the P51 and F-16 planes which use the BL17.5 and NACA 64-206 airfoils to determine which was more fuel efficient. Despite the weight and relative added complexity introduced to the aircraft by the morphing airfoil, the morphing design saved approximately 0.522 gallons of JP-8 jet fuel per mile for morphing aircraft.

TABLE III  
NACA 64-206 VALUES FROM SIMULATION AND CALCULATION

| NACA 64-206         | AOA     | Mach 0.3         | Mach 0.6          | Mach 3.5             |
|---------------------|---------|------------------|-------------------|----------------------|
| chord length [m]    |         | 1.0              | 1.0               | 1.0                  |
| lift force [N]      | 0<br>10 | 329.40<br>3747.4 | 1395.4<br>15828   | -18373.64<br>2351798 |
| drag force [N]      | 0<br>10 | 36.60<br>803.67  | 154.76<br>3396.00 | 28751.1<br>637928.30 |
| Coefficient of Lift | 0<br>10 | 0.05<br>0.06     | 0.05<br>0.06      | -0.00083<br>0.11     |
| Coefficient of Drag | 0<br>10 | 0.01<br>0.13     | 0.01<br>0.13      | 0.01<br>2.65         |

## V. CONCLUSIONS

### A. Accomplishments and Significance of Findings

The COMSOL and Ansys simulations proved the effectiveness of airfoils in their respective Mach environments. This disparity in airfoil effectiveness demonstrated the value of an amorphous airfoil. The physical model displayed that such a transitioning airfoil could be achieved with a simple mechanical process and lift/drag tests proved the extent to which this transition would improve efficiency. On a to-scale, physical aircraft, the extent to which these beneficial increases in lift and decreases in drag would only be scaled up. Employing amorphous airfoils would be invaluable to maximize efficiency in multiple environments. With this proof of concept design, the simulated morphing airfoil experienced increased lift in subsonic environments and decreased drag in supersonic environments caused by the change in airfoil geometry. In addition, the aircraft was proved to be create a more fuel efficient aircraft and the prototype provided confirmation that such a design is attainable.

### B. Future Research

The physical model of the amorphous airfoil could be improved with alternative resources. A stronger and more flexible material such as a Kevlar mixed with epoxy could expand the mechanical limits of the transition system [13]. Furthermore, aerodynamic factors such as drag on the material of the wing surface and varying airfoil thickness along the wing could be considered. Future research could experiment with different airfoil geometries. It is plausible that a pair of better paired airfoil shapes exist which may have an especially pronounced effect on lift, drag and fuel efficiency within this amorphous system that can only be determined through the use of mathematical optimization.

## VI. ACKNOWLEDGMENTS

The authors of this paper would like to thank those who allowed this research project to be successful: the Rutgers School of Engineering, Rutgers University, and the State of New Jersey Office of the Secretary of Higher Education for giving us the opportunity for further education in engineering; Lockheed Martin and other sponsors for generously funding our projects, and Governor's School of New Jersey Program in Engineering and Technology alumni and benefactors for their support and participation. It is also imperative to thank Dean

Jean Patrick Antoine, Director of Governor's School of New Jersey Program in Engineering and Technology, for his management and supervision; Project Mentor Jay Kapasiawala for his fundamental teaching and guidance; Dr. Prosenjit Bagchi, MAE Professor of Rutgers University School of Engineering, for his counseling; Residential Teaching Assistant Lasya A. Balachandran for her vital time and assistance; Research Coordinator June Lee for her support; Head Residential Teaching Assistant Ian Joshua C. Origenes for his supervision and management, and members of the Rutgers Makerspace for their invaluable aid in constructing the physical model.

## REFERENCES

- [1] J. Kapasiawala, "Amorphous Airfoil Design," Jun. 2022.
- [2] P. of Flight, "Airfoil Design (Part One)," Flight Literacy, Nov. 27, 2017. <https://www.flightliteracy.com/airfoil-design-part-one/>[https://www.nasa.gov/sites/default/files/atoms/files/2008-2009-1st-non-us-tea\\_3\\_kareas.pdf](https://www.nasa.gov/sites/default/files/atoms/files/2008-2009-1st-non-us-tea_3_kareas.pdf)
- [3] Skybrary, "Angle of Attack (AOA)," SKYbrary Aviation Safety, May 25, 2021. <https://skybrary.aero/articles/angle-attack-aoa>
- [4] K. M. Casper, J. Wagner, S. J. Beresh, J. F. Henfling, R. W. Spillers, and B. O. M. Pruett, "Complex Geometry Effects on Subsonic Cavity Flows.," [www.osti.gov](http://www.osti.gov), Dec. 01, 2014. <https://www.osti.gov/servlets/purl/1242764> (accessed Jul. 22, 2022).
- [5] M. Cho and S. Kim, "Structural morphing using two-way shape memory effect of SMA," *International Journal of Solids and Structures*, vol. 42, no. 5–6, pp. 1759–1776, Mar. 2005, doi: 10.1016/j.ijsolstr.2004.07.010
- [6] R. Calzada, "P-51D Mustang," NASA, Sep. 08, 2015. [https://www.nasa.gov/centers/dryden/multimedia/imagegallery/P-51/P-51\\_proj\\_desc.html#:text=The%20P%2D51D%20was%20the](https://www.nasa.gov/centers/dryden/multimedia/imagegallery/P-51/P-51_proj_desc.html#:text=The%20P%2D51D%20was%20the) (accessed Jul. 16, 2022)
- [7] "Aerospaceweb.org — Aircraft Museum - F-16 Fighting Falcon," [Aerospaceweb.org](http://www.aerospaceweb.org/aircraft/fighter/f16/), 2011. <http://www.aerospaceweb.org/aircraft/fighter/f16/>
- [8] "P-51D ROOT (BL17.5) AIRFOIL (p51droot-il)," [airfoiltools.com](http://airfoiltools.com). <http://airfoiltools.com/airfoil/details?airfoil=p51droot-il> (accessed Jul. 19, 2022).
- [9] "NACA 64-206 (naca64206-il)," [airfoiltools.com](http://airfoiltools.com). <http://airfoiltools.com/airfoil/details?airfoil=naca64206-il>
- [10] "X-15 Research Results: Chapter 5," [history.nasa.gov](https://history.nasa.gov/SP-60/ch-5.html). <https://history.nasa.gov/SP-60/ch-5.html>
- [11] "Wave Drag," SKYbrary Aviation Safety, May 26, 2021. <https://skybrary.aero/articles/wave-drag#:text=This%20wave%20drag%20can%20be> (accessed Jul. 21, 2022).
- [12] "Airfoil\_Efficiency" [https://github.com/AmiriHayes/Airfoil\\_Efficiency](https://github.com/AmiriHayes/Airfoil_Efficiency), July 29, 2022
- [13] T. F. Geyer and E. Sarradj, "Trailing Edge Noise of Partially Porous Airfoils," 20th AIAA/CEAS Aeroacoustics Conference, Jun. 2014, doi: 10.2514/6.2014-3039